Macromolecules

ARTICLE

pubs.acs.org/Macromolecules

Height and Width of Adsorbed Dendronized Polymers: Electron and Atomic Force Microscopy of Homologous Series

Baozhong Zhang,[†] Roger Wepf,[‡] Martin Kröger,[§] Avraham Halperin,[*,∥] and A. Dieter Schlüter[*,†]

[†]Laboratory of Polymer Chemistry, Department of Materials, ETH Zurich, Wolfgang−Pauli−Strasse 10, HCI J541, 8093 Zurich, Switzerland

[‡]EMEZ (Electron Microscopy ETH Zurich), ETH Zurich, Wolfgang−Pauli−Strasse 16, HPT D9, 8093 Zurich, Switzerland

[§]Polymer Physics, ETH Zurich, Wolfgang−Pauli−Strasse 10, HCI H 537, 8093 Zurich, Switzerland

[∥]Université Grenoble 1/CNRS, LIPhy UMR 5588, 38041 Grenoble, France

Supporting Information

ABSTRACT: The width, w, and height, h, of dendronized polymers (DPs) adsorbed onto mica and highly oriented pyrolitic graphite (HOPG) were characterized by atomic force microscopy (AFM) and electron microscopy (EM). The study utilized a homologous series of generations $g = 1-5$, hence enabling coadsorption and characterization under identical conditions and thus facilitating comparison. The w and h values, as acquired by AFM and EM on HOPG and mica are comparable and can be collapsed onto a single master curve by a constant horizontal shift of each set of points. This master curve exhibits the scaling behavior of a cylinder and supports the visual impression that DPs adsorb as weakly deformed cylinders. The h and w curves suggest a dendron density of $\rho \simeq 1.35$ to 1.45 g/cm^3. Density measurements of solutions of the "attached-to monomer" suggest $\rho \simeq 1.10$ g/cm^3. The corresponding estimates of the maximal generation of structurally perfect DP for this family is $g_{max} = 6$ to 7 and close to the currently explored range of $g = 1-5$.

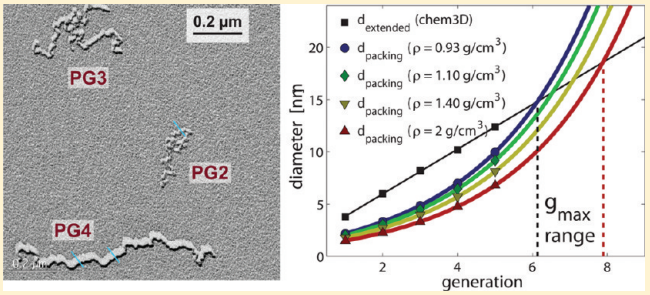

I. INTRODUCTION

Both dendronized and bottle-brush polymers comprise linear backbones carrying side chains. The side chains are linear in bottle-brushes[1−5] whereas in dendronized polymers (DPs)[6−9] they are repeatedly branched dendrons. Consequently, the side-chain coronas of the DP are denser and less deformable. Coronal deformation can be induced by adsorption onto solid substrates, and atomic force microscopy (AFM) images of bottle-brushes and DP manifest the differences in their deformability. In particular, AFM images of bottle-brushes[10−12] manifest a strong adsorption-induced flattening of the coronal chains requiring elaborate theoretical analysis.[3] In contrast, the DP images connote cylinders having comparable height, h, and width, w, both increasing with the generation, g.[13,14] The images suggest the adsorbed DP as weakly distorted cylinder. Accordingly, quantifying the g-dependent h and w is of interest as a probe of the structure and deformability of the DP corona. This is feasible because a homologous series of DPs of generations $g = 1-5$ is now available.[14] DPs that differ only in g, and thus in their thickness, exhibit similar interactions with substrates and with AFM tips. They can be accordingly coadsorbed onto a single substrate, conditions that favor comparison between DP of different g. Indeed, coadsorbed DPs of different g are easily distinguishable visually in AFM images.[13]

AFM, transmission electron microscopy (TEM), and scanning electron microscopy (SEM) all enable us to determine h and w of adsorbed DP. Of these, AFM is especially attractive because of its relative ease and wide availability. However, quantitative analysis of AFM images of DP and of macromolecules in general requires caution.[15−18] Here we note that w and h of DP are determined differently. The AFM height profile used to determine h reflects differences between the tip interactions with the substrate and with the DP, their different deformation by the tip, and so on. These effects, and others, can lead to well-documented artifacts in the measured h values. w is specified by the ridge-to-ridge distance of two coadsorbed DPs in grazing contact.[19−21] Errors in w may arise because of interpenetration of the two adjacent DP or because of contact-induced deformation.

In the following, we report h and w of DP with $g = 1-4$ obtained from AFM, SEM, and TEM for DP adsorbed onto mica, highly oriented pyrolytic graphite (HOPG), and amorphous carbon (C_{amorph}). In our analysis of the h and w data, we also include recently obtained results[14] for DP of $g = 5$. Overall, we find that the h and w values obtained by the different methods are consistent and can be superimposed upon introducing a system specific offset. In particular, the h and w values, as obtained by AFM, TEM, and SEM, can be collapsed onto a single master curve, consistent with the idea that DPs adsorb as weakly

Received: June 28, 2011
Revised: July 31, 2011
Published: August 17, 2011

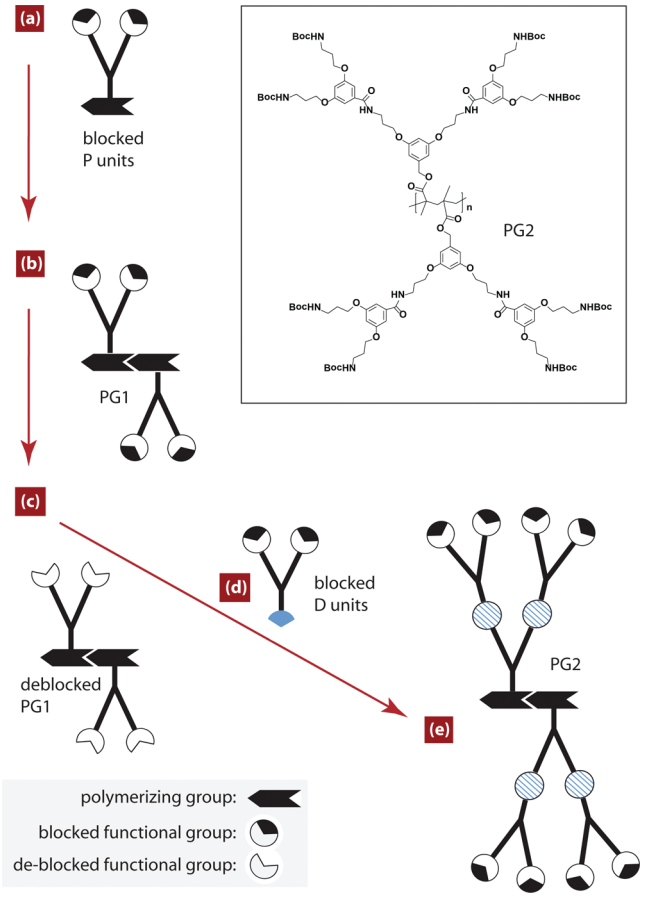

Figure 1. In the "attach to" route, P units each carrying two blocked functionalities (a) are polymerized, thus forming a $g = 1$ dendronized polymer PG1 (b). The resulting PG1 polymer is deblocked (c) and reacted with blocked D units (d) to yield a $g = 2$ dendronized polymer PG2 (e). Higher generations are created by repeating steps (c) and (d). The ChemDraw structure of PG2 is depicted in the inset, where Boc = *tert*-butyloxycarbonyl (adapted in part from ref 13).

deformed cylinders. Plots of the dendron density, ρ, as obtained upon assuming such cylindrical forms, indicate that the adsorption-induced flattening decreases with increasing g. They also yield an estimate of the density of a solvent-free corona of the DPs studied, $\rho \simeq 1.35$ to 1.45 g/cm^3. Extrapolation of measured solutions of D units (Figure 1) leads to comparable $\rho \simeq 1.10$ g/cm^3 (Supporting Information). These ρ values suggest that structurally perfect DP of this chemistry can be attained up to $g_{max} = 6-8$ and thus close to the currently explored range of $g = 1-5$.

II. MATERIALS AND METHODS

A. Polymers. Polymers with $g = 2-4$ were synthesized from a first-generation DP, $g = 1$, PG1, with two terminal amines per monomer and a number-average degree of polymerization of $P_n \approx 10\,600$. The $g = 2-4$ congeners, PG2-PG4, were obtained by a step-by-step dendronization, also known as attach-to or divergent route (Figure 1). The samples were obtained in gram quantities, and their structural perfection, as quantified by a UV labeling technique, was in every case superior to 97% (PG2: 99.4%, PG3: 98.6%, PG4: 97.1%).

B. Atomic Force Microscopy. AFM measurements were carried out with a Nanoscope IIIa multimode scanning probe microscope (Digital Instruments, San Diego, CA) operated in the tapping mode with an E scanner (scan range 10 μm × 10 μm) in air and at room temperature. The AFM utilized Olympus silicon OMCL-AC160TS cantilevers (Atomic Force F&E GmbH, Mannheim, Germany) with a resonance frequency in the 200 and 400 kHz range and a spring constant around 42 N/m. The AFM samples were prepared by spin-coating (2000 rpm) the polymer solution (3 to 4 mg/L in chloroform) onto freshly cleaved mica (PLANO W. Plannet GmbH, Wetzlar, Germany) or HOPG (Grade SPI-2, SPI Supplies, Westchester, PA). Typical measurements were carried out at resonance frequency of 300 kHz with 0.5 to 2.0 V amplitude set point and 5−90 mV drive amplitude.

C. SEM Height and Width Measurements. SEM measurements were carried utilizing a cryo-FE-SEM (Gemini 1530, Zeiss, Germany). The sample preparations for h and w measurements were different and are described below. For height measurements, DPs were absorbed by spin coating of chloroform solutions of concentration 1−10 mg/L, onto fresh cleaved mica (PLANO W. Plannet GmbH) or onto HOPG (SPI Supplies). The samples were then transferred into a freeze etching device (BAF400 Bal-Tec/Leica, Vienna, Austria), cooled to −120 °C, and shadowed with 1.5 nm of Tungsten (W) from an elevation angle of 7°. After shadowing, the samples were high-vacuum cryo-transferred to a cryo-FE-SEM chamber precooled to −120 °C for imaging. Images were taken in the SE and BSE modes at acceleration voltages of 2−10 kV and digitally recorded. h was determined from the length of the shadow in the direction of the shadowing using the trigonometric approximation $\tan \alpha = h/(\text{shadow length})$, where α is the shadowing angle.

For w measurements, DPs were adsorbed onto mica or Cu-Grid (PLANO W. Plannet GmbH) coated with a 4 nm thick amorphous carbon layer and glow discharged for 30 s prior to usage. The adsorption was carried out by contacting the grid with a 3 μL drop of DP chloroform solution (1−10 mg/L). The sample was then immediately plunge-frozen in liquid nitrogen after blotting off any excess liquid. The frozen samples were next transferred to a precooled (−140 °C) freeze etching device BAF400 (Bal-Tec, Balzers, Lichtenstein), freeze-dried at −80 °C for 2 h, and then rotary shadowed at an elevation angle of 65°, producing a 2.5 nm W coating. To preserve the 3-D hydrated structure, samples were always kept below −80 °C. The samples were loaded onto the precooled SEM cryo-stage (−120 °C) under high vacuum (VCT-100, Bal-Tec). Imaging was carried out simultaneously in the SE and BSE modes using acceleration voltages of 2−10 kV and recorded digitally. The w was measured along the normal to the DP axis and corrected for W film deposited on the DP flanks by subtracting 0.7 nm from the measured value.[22] The pixel resolution of the images was below 1 nm. Typically, 10 w values were obtained for a single chain, and the average value was used for subsequent analysis. The error bars refer to the standard deviation of the w data points.

D. TEM Height Measurements. Adsorbed DPs were prepared by spin coating of chloroform solution (1−10 mg/L) onto freshly cleaved mica (PLANO W. Plannet GmbH). The samples were transferred to a freeze etching device (BAF400 Bal-Tec/Leica) precooled to −120 °C and shadowed with 1.5 nm W from an elevation angle of 7°. The shadowed samples were then coated with an additional layer of 5−8 nm carbon to stabilize the metal film for replica production. After coating, the samples were withdrawn from the high-vacuum chamber, and the metal−carbon replica was floated onto a clean water surface. Floating pieces of the replica were then loaded onto 400-mesh Cu-TEM grids (PLANO W. Plannet GmbH) and dried in air prior to TEM investigation in a CM12 (FEI, Eindhoven, The Netherlands) at 100 kV. Images were recorded digitally with a Gatan CCD camera. h was measured as in the SEM case. Typically, 10 h values were obtained for a single chain, and the average value was used for subsequent analysis. The error bars refer to the standard deviation of the data points.

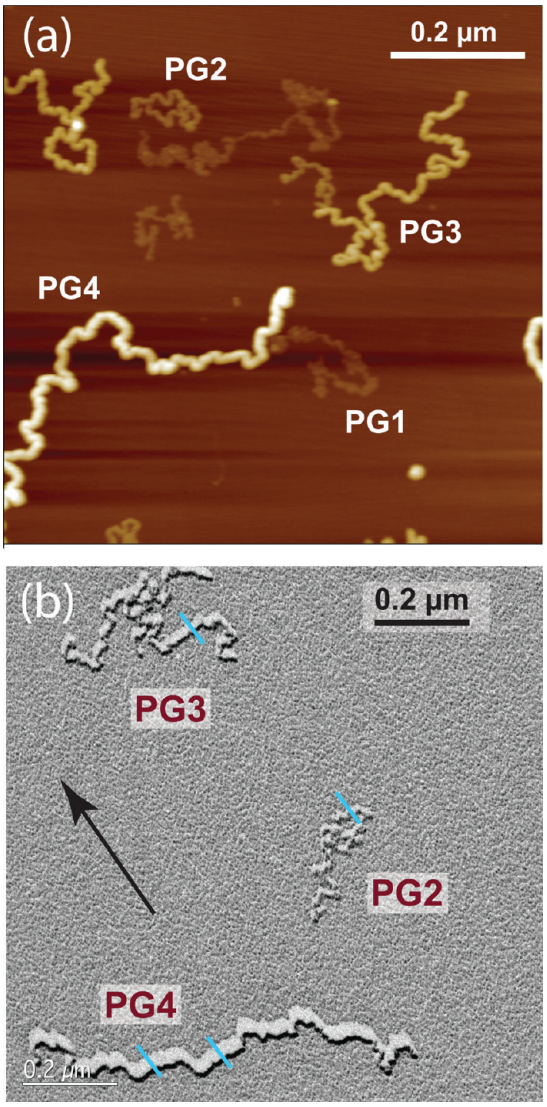

Figure 2. Selected images used for height, h, determination of coprepared PG1-PG4 chains adsorbed on mica via AFM (a) and TEM (b). All four g can be distinguished in the AFM image, whereas the PG1 chains are too thin to be observed by TEM. There is no aggregation, and the chains do not cross each other. The bars in (b) indicate some of the positions used for h analysis. (See also the Supporting Information.) The arrow indicates the direction of Tungsten shadowing.

III. RESULTS AND DISCUSSION

DP of different g can be distinguished visually in AFM and electron microscopy (EM) images because of their different thickness (Figure 2). Quantifying their h and w is, however, challenging because their values, in both AFM and EM, are acquired differently. Consequently, the h and w reported here (Tables 1 and 2) combine results obtained on different substrates and utilizing different sample preparation protocols. Yet, as we shall discuss, the h and w results are coherent despite these differences.

The AFM height, h_{AFM}, is obtained from the height profile of the polymers and is known to depend on the substrate and the humidity as well as other factors. It can vary between experiments carried out under identical conditions. The h_{AFM} values are considered with caution because they reflect the different interactions of the tip with the substrate and with the DP, possible deformation of the DP, and so on. Water condensation on the sample can also affect results.[15−18] However, h_{AFM} obtained from coadsorbed DP of different g eliminates some of these variations. AFM w values, denoted here by w_{AFM}, are specified by the ridge-to-ridge values for two chains of identical g in grazing contact.[19−21] w_{AFM} was identified with the smallest observed ridge-to-ridge distance. The measurement is only possible when such surface structures occur with sufficiently high corrugation to discriminate the two ridges. The realization of these requirements depends on the substrate, g, and the DP concentration.

Table 1. Heights in nanometers of DP g = 1−5 on Mica and HOPG[a]

h_i	substrate	g = 1	g = 2	g = 3	g = 4	g = 5
h_{AFM}	mica	0.6 ± 0.1	1.5 ± 0.1	2.3 ± 0.3	3.7 ± 0.2	6.2 ± 0.3
h_{TEM}	mica		2.3 ± 0.4	3.4 ± 0.5	4.9 ± 0.3	7.3 ± 0.2
h_{AFM}	HOPG	0.6 ± 0.2	1.6 ± 0.1	2.7 ± 0.2	4.3 ± 0.4	6.6 ± 0.4
h_{SEM}	HOPG			3.4 ± 0.3	5.4 ± 0.3	6.7 ± 0.5

[a] Values determined by AFM, SEM, and TEM are denoted by, respectively, by h_{AFM}, h_{SEM}, and h_{TEM}. The h_{AFM} on mica differ somewhat from the values reported in ref 13 because of different measuring conditions. The g = 5 values are taken from ref 14. See Figure 2 and Figure S1 of the Supporting Information for mica and Figure 3 and Figure S2 of the Supporting Information for HOPG.

Table 2. Width in nanometers of DP g = 1−5 on Mica, HOPG, and C_{amorph}[q]

w_i	substrate	g = 1	g = 2	g = 3	g = 4	g = 5
w_{AFM}	mica	1.8 ± 0.1	2.9 ± 0.4	3.9 ± 0.3	5.0 ± 0.8	7.5 ± 0.4
w_{SEM}	mica		3.1 ± 0.4	4.5 ± 0.4	6.0 ± 0.4	8.9 ± 0.5
w_{AFM}	HOPG				6.9 ± 0.5	8.6 ± 0.2
w_{SEM}	HOPG		3.5 ± 0.8	4.6 ± 0.8	7.0 ± 0.8	9.7 ± 0.8
w_{SEM}	C_{amorph}		3.1 ± 0.4	4.1 ± 0.6	6.5 ± 0.8	9.4 ± 0.3

[q] Values determined by AFM, SEM, and TEM are denoted, respectively, by w_{AFM}, w_{SEM}, and w_{TEM}. The g = 5 values are taken from ref 14. See Figure 4 and the Supporting Information.

Adsorption onto HOPG (Figure 3), a substrate with low adsorption energy, results in extended and dense submonolayer aggregates when the DP concentration is in the 1−10 mg/L range. These islands arise because of both inter- and intrachain aggregation. Islands comprising single-g DP allowed us to measure w. Islands formed by DP of different g exhibit distinctive terraces and were not used for w determination. For g = 1−3, the aggregates were not sufficiently corrugated to permit w measurements, and useful w data was obtained only for g = 4 to 5. On mica, where the adsorption is stronger, suitable surface aggregates were formed only at intermediate DP concentrations ∼30−50 mg/L (Figure 4). At high concentrations, ∼100 mg/L, the adsorbed chains are disordered and cross each other frequently. At low concentrations, ≤ 20 mg/L, grazing contacts were not obtained. Both h and w can vary along a single chain. Accordingly, the reported values are average values from ∼10 measurements.

Acquiring h and w by EM also involves distinct procedures involving different types of shadowing. Determining h requires unidirectional shadowing, whereas w is measured following

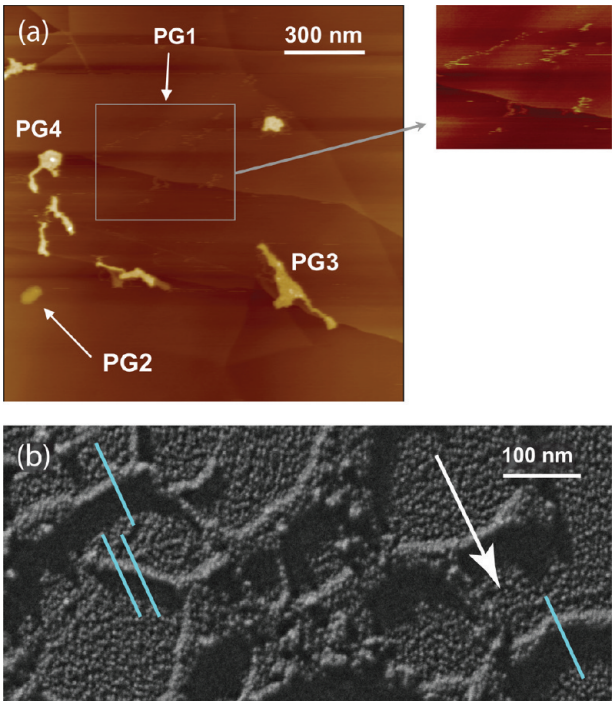

Figure 3. Selected images used for height, h, determination of DP chains ($P_n \simeq 10\,600$) adsorbed on HOPG. In contrast with the mica case (Figure 2), the chains form inter- and intrachain "islands" and cross each other. (a) AFM height image of coprepared PG1−PG4. Images with steeper color gradient (exterior frame) visualize better the PG1 chains that move laterally while being imaged. (b) Tungsten-shadowed SEM image of PG4. The bars indicate some of the positions used for h analysis. (See also Figure S2 of the Supporting Information for the corresponding images of PG3.) The arrow indicates the direction of shadowing.

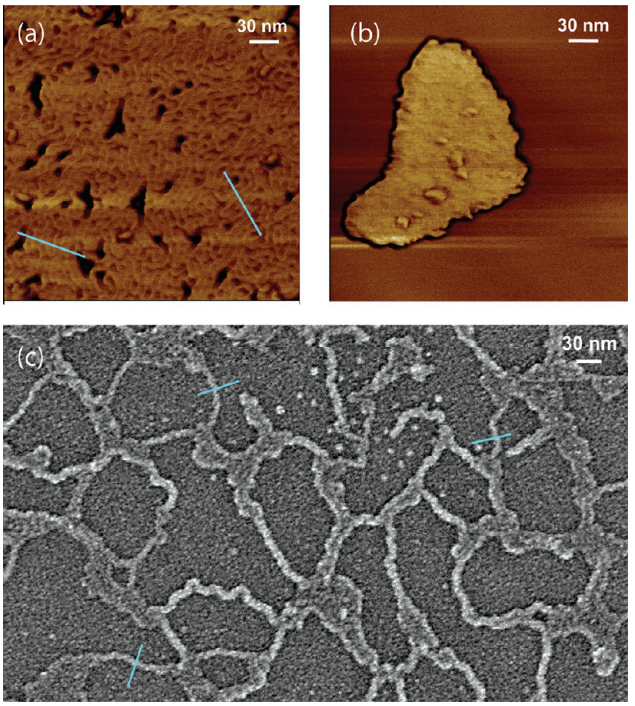

Figure 4. Selected images used for width, w, determination of DP chains (a) and (b) AFM phase images of PG3 and PG4 on HOPG. (c) SEM image of rotary shadowed PG4 adsorbed onto a 4 nm amorphous carbon film. The bars indicate some of the positions used for the w analysis. For details, see the Supporting Information.

rotary shadowing, resulting in uniform coating. For SEM, the coated specimens were used as obtained, whereas carbon replicas were used for the TEM imaging. The h and w values obtained by SEM will be denoted by h_{SEM}, w_{SEM}, and h obtained by TEM denoted by h_{TEM}. The SEM w measurement characterized the narrowest stems joining "islands". The measured h and w values are listed in Tables 1 and 2, respectively. Note that h_{AFM} is consistently lower than h_{TEM} and h_{SEM}, as previously reported.[17,18]

The h versus g plot (Figure 5a) highlights the systematic variation between the different systems and suggest that the curves can be superimposed by a lateral shift. This indeed allows us to collapse the h values as obtained by AFM, TEM and SEM onto a single curve (Figure 5b) of the form

$$h(g) + C = a\sqrt{n(g)} \tag{1}$$

where $n(g) = 2^g - 1$ is the number of repeat D branch units in dendron of generation g and a is the span of such a unit. The horizontal shift is described by C, a constant specific to a set of points labeled by the imaging method and the substrate. C allows for the differences between imaging techniques and for the unknown diameter of the $g = 0$ chain. In Figure 5b, the C values are chosen so as to superimpose the $h(g)$ curves on the scaling result, that is, eq 1 with $C = 0$ nm. It turns out that only the TEM mica set is characterized by $C = 0$ nm. The best fit for all data sets yields a characteristic length $a = 1.29$ nm related to the span of the D unit and its excluded volume parameter. As discussed below, this form is suggestive of a cylindrical object but does not allow us to distinguish among a cylinder, a hemicylinder, or an intermediate form. We emphasize that the precise cross-sectional form of the adsorbed DP is not known.

Assuming that the DPs adsorb as weakly deformed cylinders suggests that $h(g)$ is comparable to the diameter $d(g)$ of a cylinder corresponding to fully collapsed DP such that

$$d = 2\sqrt{\frac{m}{\pi\rho\delta}} \tag{2}$$

where $m(g) \approx n(g)$ is the mass of a dendron, ρ is the dendron density, and δ is the backbone contour length per dendron. Both ρ and δ may depend on g. Note that eq 2 is applicable to all g because it reflects only packing considerations. This is in contrast with results obtained for solvent swollen DP, where chain elasticity plays a role.[23] Rigorous quantitative comparison between eqs 1 and 2 is, however, difficult because of uncertainties concerning ρ and δ.

Currently there are no measurements of δ of DP. It is, however, useful to recall the results obtained in a careful study of bottle brush polymers comprising polymethacrylic backbone with every monomer carrying polystyrene side chains whose polymerization degree varied between 6 and 33.[5] Utilizing light and neutron scattering, the authors found δ 0.241 nm for toluene, a good solvent, and δ 0.207 nm for cyclohexane, a poor solvent for the side chains. These results were independent of the length of the side chains. As noted by the authors, AFM contour length measurements suggest much smaller δ values, an effect that may be attributed to small backbone undulations unresolved by AFM. Because the crowding in DP is stronger than that in

dx.doi.org/10.1021/ma2014707 |*Macromolecules* 2011, 44, 6785–6792

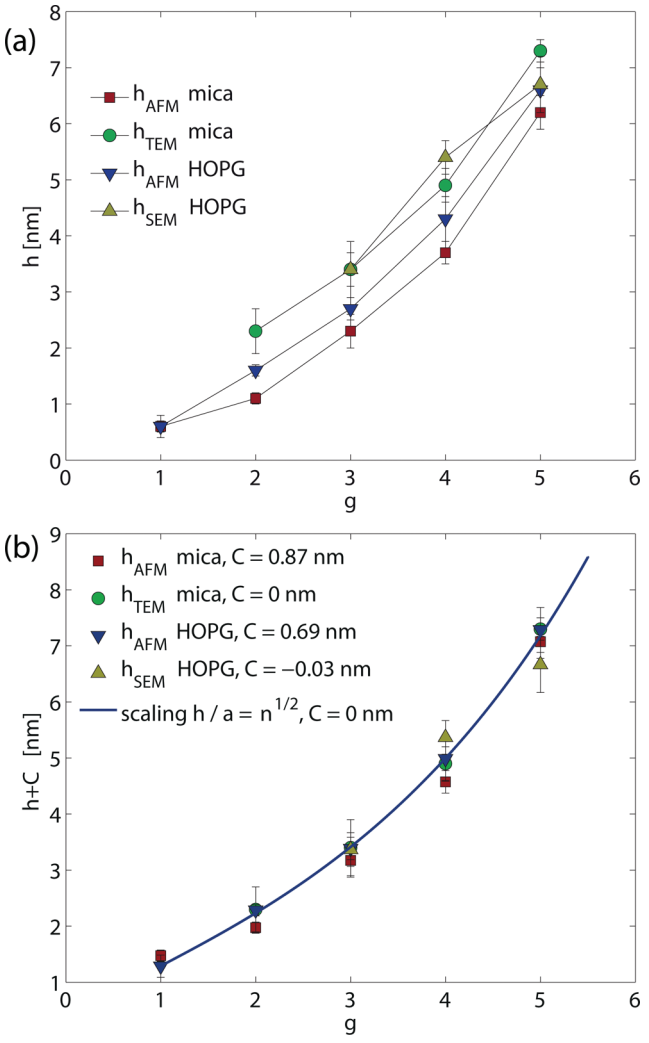

Figure 5. (a) Experimental height $h(g)$ values for PG1−PG5 adsorbed on mica and HOPG (Table 1) versus the generation g. (b) Comparison of the shifted experimental data, $h + C$, with the scaling form eq 1.

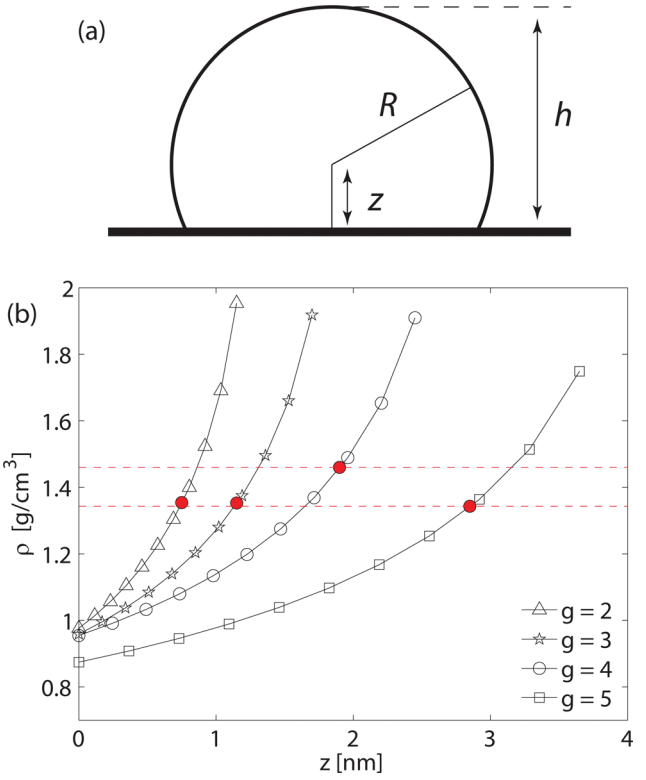

Figure 6. (b) ρ curves for a for different degrees of flattening for DP on mica of g = 2−5, as calculated (Appendix A) for the cross section depicted in part a and assuming δ = 0.25 nm. The filled red points fulfill the condition $w_{SEM} = 2R = 2(h_{TEM} - z)$, thus specifying the coronal ρm as indicated by the dashed red lines.

bottle brushes, one may expect larger δ subject to the upper bound δ = 0.25 nm corresponding to the span of two C−C bonds in an all trans configuration. δ = 0.25 nm should certainly be approached as g grows toward g_{max}, the maximal attainable g of a structurally perfect DP at the packing limit.

At the present, the ρ of DP is unknown. A rough lower estimate of $\rho(g)$ can be obtained assuming that the volume of a dendron is identical to the sum of the van der Waals volumes of the constituting atoms leading to $\rho \simeq 0.93$ g/cm^3 with negligible dependence on g. This method tends to underestimate ρ (Supporting Information). A rough upper estimate utilizes the TEM/mica measurements assuming $h = d$ and δ = 0.25 nm, thus leading to $\rho(g) = 4m/\pi n(g)a^2\delta$. For higher g values, when $n \simeq 2^g$ and $m \simeq 2n \times 175.5$ g/mol,[24] $\rho = (1404/\pi a^2\delta)$ g/mol $\simeq 1.78$ g/cm^3. This upper estimate of ρ does not allow for the deformation of the cylinder. Assuming a "flattened cylinder" form, we obtain, for each g, a ρ curve that varies with the "degree of flattening". The results depend somewhat on the assumed geometry. For the "cut circle" cross-section depicted in Figure 6a, an estimate for ρ is obtained upon identifying $w_{SEM} = 2R$, which leads to $\rho \simeq 1.35$ to 1.45 g/cm^3 (Figure 6b and Appendix A). The ρ values noted above are supplemented by extrapolation of density measurements of solutions of D monomers in dichlorobenzene (DCB) and in dimethylformamide (DMF). Whereas one of the solution density curves is increasing with the DP concentration and the other is decreasing, both lead to an extrapolated value of ρ = 1.10 g/cm^3. A previous study of related DP[25] suggests ρ = 1.2 to 1.3 g/cm^3, a typical value for aromatic polyesthers.[26]

The hypothesis that DPs adsorb as weakly deformed cylinder is also supported by plots (Figure 7) of the measured w versus the molecular weight of the dendron, m. We first stress again that the cross-sectional form of the adsorbed DP is not known in detail and that w is a rough measure of the lateral span. With this caveat in mind, most of the data points fall on a straight line, suggesting $w \simeq 1.2h$. In other words, $h < w \ll 2h$, indicating a somewhat flattened cylinder but falling short of hemicylindrical profile. Note further that the cross-sectional area A scales as $A \approx wh \approx m \approx n$.

Our microscopy results suggest that DPs adsorb as weakly deformed cylinders and yield a rough estimate of $\rho \simeq 1.35$ to 1.45 g/cm^3. Using this and the other ρ estimates listed above, one may consider the maximal attainable g for structurally perfect DPs of this family, g_{max}. The maximally extended length of a strand joining a dendron root to a free end scales as $d_{extended}/2 \approx g$, whereas packing considerations for a solvent-free corona yield $d_{packing} \approx n^{1/2}(g)$. The two curves cross at g_{max}, where the strands attain their maximal extension, thus ruling out structurally perfect DPs with $g > g_{max}$. The $d_{extended}$ values for the dendron chemistry utilized were obtained by Chem3D extension and can be fitted by $d_{extended}(g) = 2 \times (0.85 + 1.07g)$ nm. Figure 8 depicts $d_{extended}(g)$ and a family of $d_{packing}(g)$ curves as obtained from eq 2 using the

dx.doi.org/10.1021/ma2014707 |Macromolecules 2011, 44, 6785–6792

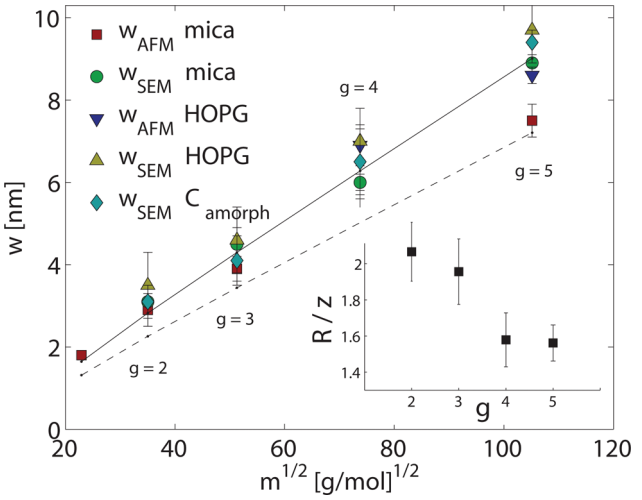

Figure 7. Experimental width, w, data (Table 2) versus square root of molecular weight m.[24] Two lines are included to guide the eye. $w = h_{AFM}$ as realized by a perfect cylinder (broken line) and $w = 1.2 \times h_{AFM}$ corresponding to a flattened cylinder (solid line). The inset shows the degree of flattening R/z versus g for $2R = w_{SEM}$ (mica) assuming a cut circle profile (Figure 6a). The relationship $w = 1.2 \times h$ corresponds to a g-independent $R/z = 1.5$ (Appendix A).

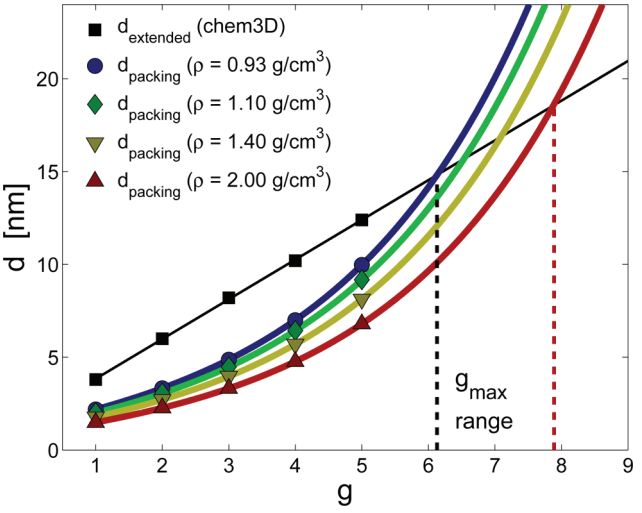

Figure 8. Maximal generation for high-fidelity DP, g_{max}, is obtained when the diameter of a densely packed DP, $d_{packing} \approx n^{1/2}(g)$, equals twice the maximal extension of a g-generation strand, $d_{extended} \approx g$. The plot depicts the linear $d_{extended} \approx g$ and various $d_{packing} \approx n^{1/2}(g)$ obtained for different ρ values discussed in the text. g_{max} for a given ρ is specified by the intersection of $d_{extended}$ with $d_{packing}$ corresponding to this ρ. The upper and lower values of g_{max} are indicated by vertical broken lines bracketing the $6.1 \leq g_{max} \leq 7.9$ range.

various ρ estimates in the range of 0.9 to 1.4 g/cm^3 previously discussed. The intersections specify the corresponding g_{max} values spanning the range of $6.1 < g_{max} < 7.1$ with g_{max} weakly increasing with the assumed ρ. Known densities of linear chains comprising C, H, O, and N suggest $\rho < 2$ g/cm^3.[27] Even allowing for very high $\rho = 2$ g/cm^3 broadens the accessible range only to $6.1 < g_{max} < 7.9$. This simple analysis implies that g_{max} of high fidelity DP of this family is close to the explored range of $g = 1-5$. A more precise value of g_{max} is at the limit of this simple approach.

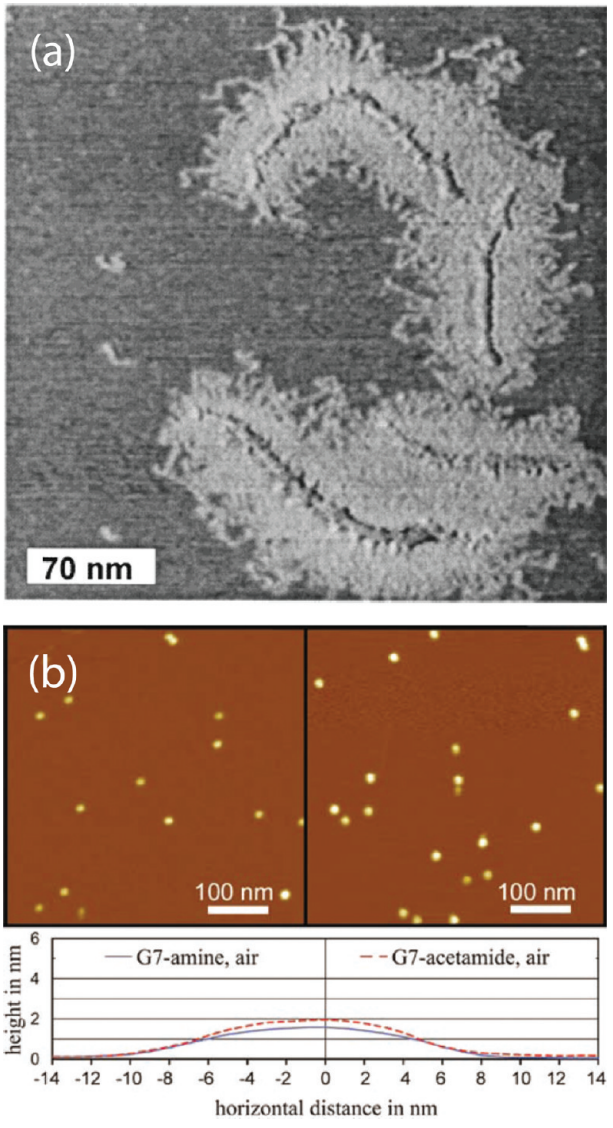

Figure 9. AFM images illustrating the deformability of (a) bottle brushes[10] and (b) dendrimers.[28]

With this reservation in mind, the following points merit consideration. Because the van der Waals estimates leading to $\rho \simeq 0.93$ g/cm^3 usually underestimate ρ (Supporting Information), this analysis suggests that high-fidelity $g = 6$ DPs are attainable. Our discussion concerns DP of high structural perfection thus having integer g values, and as a result, $g_{max} \leq 7.9$, as obtained for the high end $\rho = 2$, implies $g_{max} = 7$. The experimental feasibility of $g = 7$ dendrons depends on the precise value of ρ: It is ruled out by $\rho \simeq 1.10$ g/cm^3 but may be reachable if $\rho \simeq 1.35$ to 1.45 g/cm^3 is closer to reality. For trifunctional dendrimers of this family, g_{max} is obtained from $\pi d^3_{extended}/6 \approx 3 \times 350.4 \times n(g)/\rho$, thus leading, as expected, to a higher g_{max} in the range $12.7 < g_{max} < 14.1$. Better characterization of ρ will thus be helpful in guiding future synthetic efforts in this area.

Our results quantitatively support previous observations indicating that DPs adsorb as weakly deformed cylinders. This weak deformability distinguishes DP from dendrimers[28−32] and bottle brushes[10−12] (Figure 9). Adsorption of poly(amidoamine) dendrimers on mica has been studied by atomistic MD calculations of $g = 2-5$ and AFM measurements of $g = 5-7$. The MD study

dx.doi.org/10.1021/ma2014707 |*Macromolecules* 2011, 44, 6785–6792

lead the authors to conclude that "the dendrimers are shown to be highly flexible and capable of forming very flat structures with little free volume left inside the polymer"[28] whereas the AFM measurements suggested that "the heights of the molecules as determined by AFM are much less than the diameter in their spherically symmetric state".[28] Qualitatively similar results were obtained in AFM measurements of $g = 9$ poly(amidoamine) dendrimers at the liquid/solid interface. These lead to average height of $h = 4.7$ nm and a full width at half-maximum height of $w = 12.3$ nm, thus indicating considerable flattening.[33] Analogous behavior was observed in adsorbed hyperbranched polymers[34,35] This difference in deformability is traceable to geometry effects. Dendrimers are spherical brushes where repeatedly branched dendrons replace the linear branches found in star polymers. Similarly, DP is a cylindrical brush formed by dendrons rather than linear chains. The volume available to a side chain, be it dendron or linear chain, is smaller in a cylinder, thus leading to stronger stretching and weaker deformability. Adsorption of bottle brushes of linear chains on mica leads to strong coronal deformation, as seen in AFM images[10−12] supported by recent theoretical analysis.[3] Such bottle-brushes, like DP, are forms of cylindrical brushes, and the differences in deformability are due to the stronger stretching in DP where the side chains are repeatedly branched. We finally note that adsorption of bottle brushes can lead to chain scission, although we did not observe a similar effect in DP.[36]

The effect of adsorption on DP differs qualitatively from the bottle brush and dendrimer counterparts. It is, however, somewhat similar to the adsorption effect on tobacco mosaic virus (TMV). In a solution, the virus is a hollow cylindrical tube with outer and inner radii of 9 and 2 nm. Its structure on strongly adsorbing SiO_x surfaces was studied by small-angle X-ray scattering (SAXS) and grazing incidence small-angle X-ray scattering (GISAXS).[37] Whereas the width is essentially unmodified, the height decreases because of the collapse of the inner cavity leading to $h/w \approx 0.57$. AFM measurements indicate that h changes with the substrate and the pH. Values as low as 10 nm were reported and attributed to adsorption-induced distortion.[38] Therefore, TMV, like DP, adsorbs as a distorted cylinder, although its distortion is stronger for the surfaces studied. Similar rod-like forms are observed in adsorbed core−shell bottle brushes with cross-linked shells.[39]

IV. CONCLUSIONS

Imaging of adsorbed DP suggests cylindrical form with comparable h and w. However, the majority of the previously reported results were obtained by AFM, and their interpretation is difficult because of well-documented artifacts associated with this technique. To gain a better understanding of DP adsorption, we studied h and w of DP adsorbed onto mica and HOPG utilizing both EM and AFM. In our study, we utilized a homologous series of DP with $g = 1-5$ coadsorbed onto the same surface. The measured results were thus obtained under identical conditions, allowing us to eliminate spurious effects that occur when each DP is adsorbed separately. Importantly, this procedure is possible because of two distinctive features of DP: (i) AFM and EM allow us to distinguish between DPs of different g because of their different thickness and (ii) all members of the homologous series exhibit similar interactions and can be coadsorbed onto the same substrate under identical conditions. The use of homologous series is important for two additional reasons. First, the interactions between the AFM tip and the DP of different g are comparable. Second, the homologous series affords a "tuning parameter", g, which does not exist when studying the adsorption of "single thickness" polymers such as DNA. Therefore, one may analyze the variation of h and w as a function of g and compare it with theoretical expectations.

Our results support the suggestion that DPs adsorb as weakly deformed cylinders though the degree of deformation varies with g. Their flattening weakens as g grows. Importantly, the EM and AFM results can be superimposed by horizontally shifting data sets obtained for a specific surface and microscopy technique. The resulting $h(g)$ and $w(g)$ plots exhibit $n^{1/2}$ scaling as expected for adsorbed cylinders. We stress, however, that this scaling is expected from a family of cross sections including, for example, hemicylinders. We should add that our observations concern mica and HOPG surfaces and different behavior may occur at different substrates.

Analysis of the h and w data suggests $\rho \simeq 1.35$ to 1.45 g/cm^3. Extrapolation of density measurements of solutions of D monomers in DMF and DCB leads to a lower estimate of $\rho \simeq 1.10$ g/cm^3. Altogether, the ρ values suggest $6.5 \leq g_{max} \leq 7.1$. The estimated g_{max} range broadens somewhat if one uses the van der Waals $\rho \simeq 0.78$ g/cm^3 and the high end $\rho \simeq 2.0$ g/cm^3, thus leading to $6.1 < g_{max} \leq 7.9$. Importantly, all g_{max} estimates are close to the currently explored range of $g = 1-5$.

The coronal deformation of adsorbed DP is lower than that of dendrimers because the cylindrical geometry of the DP provides lower volume per dendron, thus giving rise to stronger chain stretching. Bottle brushes of linear chains are more deformable than DP comprising repeatedly branched dendrons because the strands in the highly crowded DP are closer to their maximum extension. These arguments suggest that DP with $g > 5$ will exhibit less deformable coronas and possess higher backbone rigidity. The synthesis of DP with $g > 5$ is, however, expected to face difficulties as g_{max} is approached because of decreasing accessibility of the reactive free ends and solubility problems. The feasibility of $g > 5$ remains to be explored.

APPENDIX A: ρ FOR A FLATTENED CYLINDER

To calculate ρ for each experimental measurement point without using the fitting parameters a and C, we assume a cut circle profile (Figure 6a) of variable radius R whose center resides at a distance $0 \leq z \leq h/2$ above the surface and whose highest point equals $h = z + R$. For $z = h/2$, this form corresponds to a circular cross-section, and for $z = 0$, this corresponds to a hemicircle. The density of a dendron of volume $V(z)$ is

$$\rho(z) = \frac{m(g)}{V(z)} = \frac{m(g)}{A(z)\delta} \tag{A1}$$

where the area of a cut circle is

$$A(z) = \frac{\pi}{2}R^2 + 2\int_0^z \sqrt{R^2 - x^2}\, dx$$
$$= R^2(\pi + Z\sqrt{1 - Z^2} - \cos^{-1} Z) \tag{A2}$$

Here $Z \equiv z/R$ and $R = h - z$. $\rho(z)$ is thus estimated from eqs A1 and A2 for each g using the measured heights h, the known $m(g)$,[24] and assuming $\delta = 0.25$ nm (Figure 6b). The known width $w = 2R$ and h are used to obtain a z value for each g via $z/w = h/w - 1/2$ (filled red circles in Figure 6b). The degree of flattening can also be expressed in terms of the width-to-height ratio, $R/z = \gamma/(2 - \gamma)$ with $\gamma \equiv w/h$.

dx.doi.org/10.1021/ma2014707 |Macromolecules 2011, 44, 6785–6792

■ ASSOCIATED CONTENT

Supporting Information. AFM, SEM, and TEM images, structures of simplified PG1-5 calculated by chem 3D (MM2), reversed-color, zoomed-in SEM image of PG1-4 on HOPG, solution density measurements of G1 and the extrapolation to bulk density, chemical structure of G1 dendron, calculated and real bulk density of polymers, and references. This material is available free of charge via the Internet at http://pubs.acs.org.

■ ACKNOWLEDGMENT

This work was financially supported by the Swiss National Science Foundation (NRP 62 "Smart Materials"), which is gratefully acknowledged. We thank Profs. N. D. Spencer and M. Textor, ETHZ, for the access to the AFM.

■ REFERENCES

(1) Rahlwes, D.; Roovers, J. E. L.; Bywater, S. *Macromolecules* **1977**, *10*, 604.

(2) Hsieh, H. L.; Quirk, R. P. In *Anionic Polymerization. Principle and Practical Applications*; Hudgin, D. E., Ed.; Marcel Dekker: New York, 1996.

(3) Panyukov, S.; Zhulina, E. B.; Sheiko, S. S.; Randall, G. C.; Brock, J.; Rubinstein, M. *J. Phys. Chem. B* **2009**, *113*, 3750–3768.

(4) Theodorakis, P. E.; Paul, W.; Binder, K. *Europhys. Lett.* **2009**, *88*, 63002.

(5) Zhang, B.; Gröhn, F.; Pedersen, J. S.; Fischer, K.; Schmidt, M. *Macromolecules* **2006**, *39*, 8440–8450.

(6) Schlüter, A. D.; Rabe, J. P. *Angew. Chem., Int. Ed.* **2000**, *39*, 864–883.

(7) Schlüter, A. D. *Top. Curr. Chem.* **2005**, *245*, 151–191.

(8) Frauenrath, H. *Prog. Polym. Sci.* **2005**, *30*, 325–384.

(9) Rosen, B. M.; Wilson, C. J.; Wilson, D. A.; Peterca, M.; Imam, M. R.; Percec, V. *Chem. Rev.* **2009**, *109*, 6275–6540.

(10) Sheiko, S. S.; Prokhorova, S. A.; Beers, K. L.; Matyjaszewski, K.; Potemkin, I. I.; Khokhlov, A. R.; Moller, M. *Macromolecules* **2001**, *34*, 8354–8360.

(11) Sheiko, S. S.; Moller, M. *Chem. Rev.* **2001**, *101*, 4099–4123.

(12) Pyun, J.; Kowalewski, T.; Matyjaszewski, K. *Macromol. Rapid Commun.* **2003**, *24*, 1043–1059.

(13) Guo, Y.; van Beek, J. D.; Zhang, B.; Colussi, M.; Walde, P.; Zhang, A.; Kröger, M.; Halperin, A.; Schlüter, A. D. *J. Am. Chem. Soc.* **2009**, *131*, 11841–11854. Note that this publication reports $P_n \sim 7000$ for the exact same polymer PG1. This result is based on GPC measurements using polystyrene standards. In a later study, the actual molar mass was determined to be $P_n \approx 12\,600$ by dynamic light scattering.[14]

(14) Zhang, B.; Wepf, R.; Fischer, K.; Schmidt, M.; Besse, S.; Lindner, P; King, B. T.; Sigel, R.; Schurtenberger, P.; Talmon, Y.; Ding, Y.; Kröger, M.; Halperin, A.; Schlüter, A. D. *Angew. Chem., Int. Ed.* **2011**, *123*, 763–766.

(15) Beaglehole, D.; Christenson, H. K. *J. Phys. Chem.* **1992**, *96*, 3359–3403.

(16) Yang, G.; Vesenka, J. P.; Bustamante, C. *J. Scanning* **1996**, *18*, 344–350.

(17) Van Noort, S. J. T.; Van der Werf, K. O.; De Grooth, B. G.; Van Hulst, N. F.; Greve, J. *Ultramicroscopy* **1997**, *69*, 117–127.

(18) Zhuang, W.; Ecker, C.; Metselaar, G. A.; Rowan, A. E.; Nolte, R. J. M.; Samori, P.; Rabe, J. P. *Macromolecules* **2005**, *38*, 473–480.

(19) Stocker, W.; Schürmann, B. L.; Rabe, J. P.; Förster, S.; Lindner, P.; Neubert, I.; Schlüter, A. D. *Adv. Mater.* **1998**, *10*, 793–797.

(20) Percec, V.; Ahn, C.-H.; Ungar, G.; Yeardley, D. J. P.; Möller, M.; Sheiko, S. S. *Nature* **1998**, *391*, 161–164.

(21) Ecker, C.; Severin, N.; Shu, L.; Schlüter, A. D.; Rabe, J. P. *Macromolecules* **2004**, *37*, 2484–2489.

(22) Winkler, H. *Computerunterstützte Interpretation elektronenmikroskopischer Bilder von dekorierten und beschatteten biologischen Oberflächen*, ETH Diss. Nr. 8186, ETH Zurich, 1986.

(23) Halperin, A.; Peleg, O.; Kröger, M. *Macromolecules* **2010**, *43*, 6213–6224. Results for DPs are summarized in row 6 of Table 1, cf. column 3 for the poor solvent case used here to describe the AFM/SEM results.

(24) A single dendron is composed of NH = $26 \times 2^g - 10$ hydrogen, NC = $18 \times 2^g - 9$ carbon, NO = $5 \times 2^g - 2$ oxygen, and NN = $2 \times 2^g - 2$ nitrogen atoms. The dendron mass is thus $m(g) = 2 \times (175 \times 2^g - 89)$ g/mol, and the total number of atoms is $n_a(g) = 51 \times 2^g - 23$, whereas the total number of branch units is $n(g) = 2^g - 1$. The mean mass per atom quickly approaches $m/n_a \approx 6.8$ g/mol with increasing g, and the mean mass per branch unit is $m/n \approx 351$ g/mol.

(25) Förster, S.; Neubert, I.; Schlüter, A. D.; Lindner, P. *Macromolecules* **1999**, *32*, 4043–4049.

(26) Brydson, J. A. *Plastic Materials*, 6th ed.; Butterworth & Heinemann: Oxford, U.K., 1995.

(27) *Polymer Handbook*, 3rd ed.; Brandrup, J.; Immergut, E. H., Eds.; J. Wiley: New York, 1989; Chapter V.

(28) Mecke, A.; Lee, I.; Baker, J. R., Jr.; Banaszak Holl, M. M.; Orr, B. G. *Eur. Phys. J. E* **2004**, *14*, 7–16.

(29) Mansfield, M. L. *Polymer* **1996**, *37*, 3835–3641.

(30) Sheiko, S. S.; Eckert, G.; Ignatéva, G.; Muzafarov, A. M.; Spickermann, J.; Räder, H. J.; Möller, M. *Macromol. Rapid Commun.* **1996**, *17*, 283–297.

(31) Bliznyuk, V. N.; Rinderspacher, F.; Tsukruk, V. V. *Polym. Commun.* **1998**, *39*, 5249–5252.

(32) Li, J.; Piehler, L. T.; Qin, D.; Baker, J. R., Jr.; Tomalia, D. A. *Langmuir* **2000**, *16*, 5613–5616.

(33) Müller, T.; Yablon, D. G.; Karchner, T.; Knapp, D.; Kleinmann, M. H.; Fang, H.; Durning, C. J.; Tomalia, D. A.; Turro, N. J.; Flynn, G. W. *Langmuir* **2002**, *18*, 7452–7455.

(34) Shulha, H.; Zhai, X.; Tsukruk, V. V. *Macromolecules* **2003**, *36*, 2825–2831.

(35) Sidorenko, A.; Zhai, X. W.; Peleshanko, S.; Greco, A.; Shevchenko, V. V.; Tsukruk, V. V. *Langmuir* **2001**, *17*, 5924–5931.

(36) Sheiko, S. S.; Sun, F. C.; Randall, A.; Shirvanyants, D.; Rubinstein, M.; Lee, H.-i.; Matyjaszewski, K. *Nature* **2006**, *440*, 191–194.

(37) Lee, B.; Lo, C.-T.; Thiyagarajan, P.; Winans, R. E.; Li, X.; Niu, Z.; Wang, Q. *Langmuir* **2007**, *23*, 11157–11163.

(38) Knez, M.; Sumser, M. P.; Bittner, A. M.; Wege, C.; Jeske, H.; Hoffmann, D. M. P.; Kuhnke, K.; Kern, K. *Langmuir* **2004**, *20*, 441–447.

(39) Huang, K.; Rzayev, J. *J. Am. Chem. Soc.* **2009**, *131*, 6880–6885.